Hydrogen peroxide differentially modulates cardiac myocyte nitric oxide synthesis

Juliano L. Sartoretto[a], Hermann Kalwa[a], Michael D. Pluth[b,1], Stephen J. Lippard[b], and Thomas Michel[a,2]

[a]Cardiovascular Division, Department of Medicine, Brigham and Women's Hospital, Harvard Medical School, Boston, MA 02115; and
[b]Department of Chemistry, Massachusetts Institute of Technology, Cambridge, MA 02139

Edited by Carl F. Nathan, Weill Medical College of Cornell University, New York, NY, and approved August 2, 2011 (received for review July 14, 2011)

Nitric oxide (NO) and hydrogen peroxide (H_2O_2) are synthesized within cardiac myocytes and play key roles in modulating cardiovascular signaling. Cardiac myocytes contain both the endothelial (eNOS) and neuronal (nNOS) NO synthases, but the differential roles of these NOS isoforms and the interplay of reactive oxygen species and reactive nitrogen species in cardiac signaling pathways are poorly understood. Using a recently developed NO chemical sensor [Cu_2(FL2E)] to study adult cardiac myocytes from wild-type, $eNOS^{null}$, and $nNOS^{null}$ mice, we discovered that physiological concentrations of H_2O_2 activate eNOS but not nNOS. H_2O_2-stimulated eNOS activation depends on phosphorylation of both the AMP-activated protein kinase and kinase Akt, and leads to the robust phosphorylation of eNOS. Cardiac myocytes isolated from mice infected with lentivirus expressing the recently developed H_2O_2 biosensor HyPer2 show marked H_2O_2 synthesis when stimulated by angiotensin II, but not following β-adrenergic receptor activation. We discovered that the angiotensin-II-promoted increase in cardiac myocyte contractility is dependent on H_2O_2, whereas β-adrenergic contractile responses occur independently of H_2O_2 signaling. These studies establish differential roles for H_2O_2 in control of cardiac contractility and receptor-dependent NOS activation in the heart, and they identify new points for modulation of NO signaling responses by oxidant stress.

nitric oxide synthase | signal transduction | angiotensin II | biosensors

Cell-derived reactive oxygen species (ROS) oxidize a broad array of biomolecules and are implicated in pathological states ranging from neurodegeneration to atherosclerosis (1, 2). However, not all effects of ROS are deleterious. Endogenously generated ROS have been implicated in posttranslational protein modifications that subserve critical roles in cellular signaling (3). Hydrogen peroxide (H_2O_2) is one such ROS that has recently been identified as a key physiological signaling molecule in many cell types (4, 5).

The physiological role of H_2O_2 in the heart is incompletely understood, and little is known about the interplay between H_2O_2 and the reactive nitrogen species NO. NO is an important signaling molecule (6, 7) and plays key roles in modulating cardiac myocyte function (8). The endothelial isoform of nitric oxide synthase (eNOS) is robustly expressed under physiological conditions in cardiac myocytes, where the neuronal NOS isoform (nNOS) is also present. Diverse cell surface receptor-modulated pathways activate eNOS, and other extracellular stimuli enhance H_2O_2 synthesis, but the relationships between NO and H_2O_2 in cardiac myocyte signaling are incompletely characterized.

Results and Discussion

Here we studied NO and H_2O_2 synthetic pathways in cardiac myocytes isolated from adult mice. Using a highly sensitive fluorescent probe Cu_2(FL2E) (9, 10) to visualize NO production in these cells, we discovered that low concentrations of H_2O_2 (*ca.* 10 μM) promote robust NO synthesis (Fig. 1). The principal NOS isoform in cardiac myocytes, eNOS, is a phosphoprotein that undergoes phosphorylation on multiple residues. We found that H_2O_2 treatment increases myocyte eNOS phosphorylation on serine residues 1177 and 633 (Fig. 1 *B* and *C*), sites associated with eNOS enzyme activation (11). The increase in eNOS phosphorylation at these sites occurs at concentrations of added H_2O_2 that are within the physiological range (4).

Several protein kinases phosphorylate eNOS (see review in Dudzinski et al., ref. 11), including the AMP-activated protein kinase (AMPK), which phosphorylates the enzyme on serine 1177 in cardiac myocytes (12) and on serine 633 in vascular endothelial cells (13). AMPK has been implicated in control of cardiac metabolism and hypertrophy; less is known about the cardiac significance of drugs that may modify AMPK pathways. In addition to its archetypal activator AMP, AMPK can be activated by diverse agonist-modulated protein kinases (12–14), some of which are affected by cellular levels of AMP, whereas others are activated by calcium-dependent pathways. Kinase Akt phosphorylates eNOS on serine 1177 in endothelial cells and cardiac myocytes. In vascular endothelial cells, H_2O_2 has been documented to promote eNOS phosphorylation via AMPK (1, 14) or kinase Akt (15) pathways, associated with increases in eNOS activity (16). We found that H_2O_2 stimulates AMPK phosphorylation in cardiac myocytes with a time course similar to that seen for H_2O_2-stimulated eNOS phosphorylation (Fig. S1*A*). We used protein kinase inhibitors to explore the phosphorylation pathways stimulated by H_2O_2; RNA interference methods have not been feasible in these cells. We found that the AMPK inhibitor compound C (17) blocks H_2O_2-promoted eNOS phosphorylation at serine 633 and serine 1177 residues (Fig. 1*D*). H_2O_2 also increases phosphorylation of kinase Akt with a time course similar to that seen for H_2O_2-stimulated eNOS and AMPK phosphorylations (Fig. S1*B*). Inhibition of AMPK by compound C reduces the H_2O_2-promoted increase in Akt phosphorylation (Fig. S1*C*), suggesting that AMPK may lie upstream of Akt, as previously shown in vascular endothelial cells (14). The specificity of compound C as an AMPK inhibitor has been previously validated (17), and we found that compound C does not affect mitogen-activated protein kinase kinase (MEK) or ERK1/2 phosphorylations. Both the PI3K inhibitor wortmannin and Akt inhibitor XI block the H_2O_2-promoted eNOS phosphorylation at Ser^{633} and Ser^{1177} residues, but these inhibitors do not attenuate H_2O_2-promoted AMPK phosphorylation (Fig. 1*E* and Fig. S1 *D* and *E*). These observations identify AMPK and Akt as critical determinants of H_2O_2-promoted eNOS phosphorylation in cardiac myocytes.

Cellular imaging of cardiac myocytes treated with H_2O_2 revealed an increase in eNOS serine 1177 phosphorylation at internal membrane sites (Fig. 2*A*), consistent with the known subcellular distribution of eNOS when phosphorylated at this

Author contributions: J.L.S., H.K., M.D.P., S.J.L., and T.M. designed research; J.L.S., H.K., and M.D.P. performed research; H.K., M.D.P., and S.J.L. contributed new reagents/analytic tools; J.L.S., H.K., M.D.P., S.J.L., and T.M. analyzed data; and J.L.S. and T.M. wrote the paper.

The authors declare no conflict of interest.

This article is a PNAS Direct Submission.

[1]Present address: Department of Chemistry, University of Oregon, Eugene, OR 97403.

[2]To whom correspondence should be addressed. E-mail: thomas_michel@harvard.edu.

This article contains supporting information online at www.pnas.org/lookup/suppl/doi:10.1073/pnas.1111331108/-/DCSupplemental.

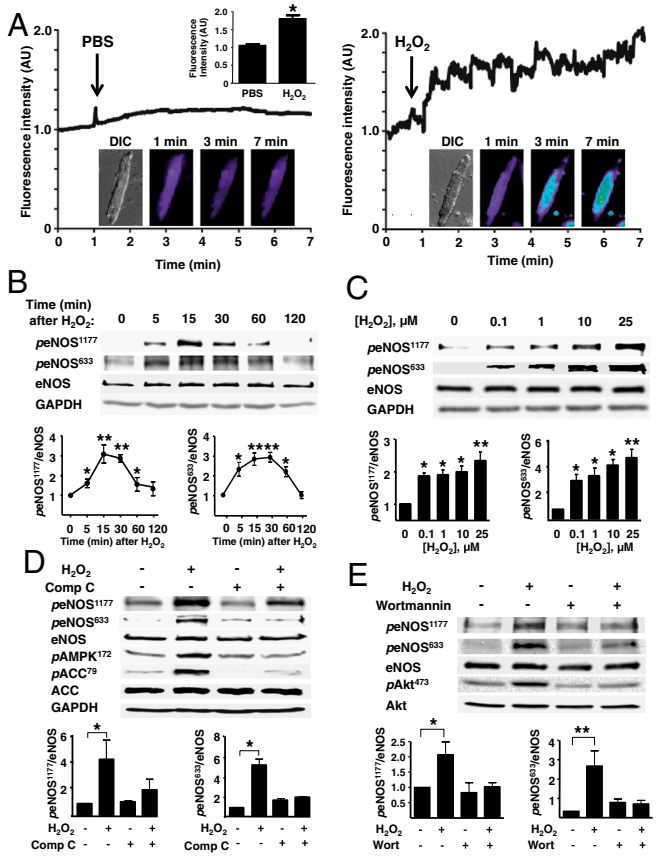

Fig. 1. Effects of H_2O_2 on cardiac myocyte NO synthesis and eNOS phosphorylation. (*A*) Adult mouse cardiac myocytes were loaded with the NO dye Cu_2(FL2E), and then treated either with PBS or H_2O_2 (10 μM). Fluorescence tracings are shown from a typical experiment, as well as representative differential interference contrast (DIC) and fluorescence images (1, 3, and 7 min). AU, arbitrary units. (*B* and *C*) Representative immunoblots from time course (*B*) or dose-response (*C*) experiments documenting the effects of H_2O_2 on eNOS phosphorylation at Ser1177 (peNOS^{1177}) or Ser633 (peNOS^{633}). (*D*) Cardiac myocytes were incubated with compound C (Comp C, 20 μM, 30 min) or vehicle, then treated with H_2O_2 and analyzed in immunoblots probed with antibodies as shown. (*E*) Immunoblot analyses from cardiac myocytes incubated with the PI3-kinase inhibitor wortmannin (1 μM, 30 min) or vehicle, then treated with H_2O_2. Below each representative immunoblot are shown the results of densitometric analyses from pooled data, documenting the changes in peNOS^{1177} and peNOS^{633} plotted relative to the signals present in unstimulated cells. Each data point represents the mean ± SE derived from at least three independent experiments; * indicates $p < 0.05$ and ** indicates $p < 0.01$.

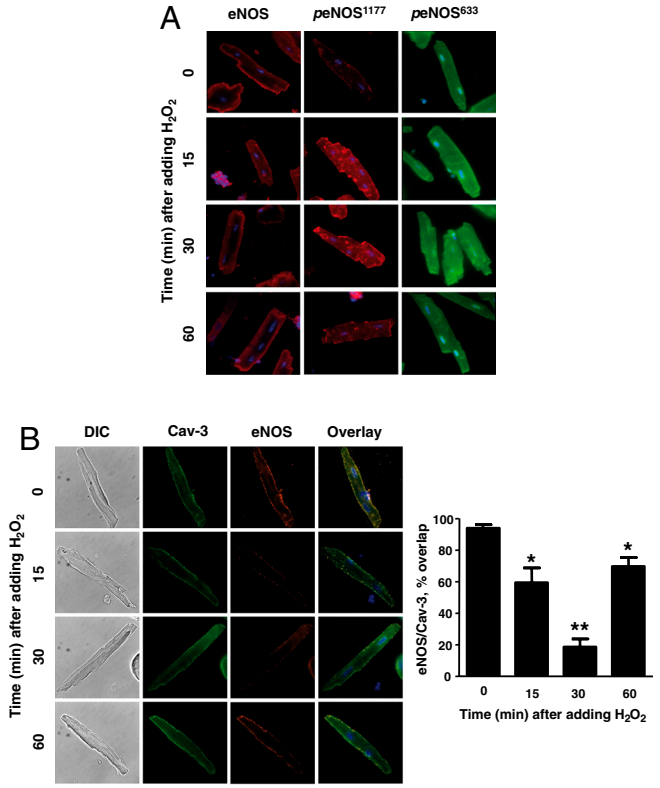

Fig. 2. H_2O_2-promoted eNOS phosphorylation and translocation in cardiac myocytes. (*A*) Results of immunohistochemical analyses of cardiac myocytes that were treated with H_2O_2 (10 μM) for the indicated times, and then fixed, permeabilized, probed with antibodies against total eNOS, peNOS Ser^{1177}, or peNOS Ser^{633}, and imaged using confocal microscopy. (*B*) Images of cardiac myocytes treated with H_2O_2 (10 μM) for the indicated times and then fixed, permeabilized, and probed with antibodies against total eNOS (Alexa Fluor red 568) or Cav-3 (Alexa Fluor green 488); overlapping signals are shown in yellow. The images shown on the left are representative of three independent experiments that yielded similar results; the bar graph on the right shows pooled data from three experiments, quantitating the percent overlap between eNOS and Cav-3 at different times after adding H_2O_2; * indicates $p < 0.05$; ** indicates $p < 0.01$ compared to $t = 0$.

residue (18). The H_2O_2-promoted increase in eNOS phosphorylation at serine 633 is not restricted to intracellular membranes (Fig. 2*A*). Because eNOS undergoes intracellular translocation following enzyme activation (11), we explored the association between eNOS and caveolin 3, a binding partner of eNOS in cardiac myocytes (19, 20). Caveolin 3 also serves as a marker for the microdomains known as plasmalemmal caveolae. As shown in Fig. 2*B*, prior to the addition of H_2O_2, eNOS and caveolin 3 are colocalized in cardiac myocytes. After adding H_2O_2, eNOS translocated from peripheral membranes to intracellular sites; the enzyme then returned to the peripheral membrane an hour after addition of H_2O_2. The colocalization between eNOS and caveolin 3 undergoes a striking decrease following the addition of H_2O_2; the return of eNOS to peripheral membranes is associated with an increase in eNOS-caveolin-3 colocalization. These findings reveal that low concentrations of H_2O_2 promote a striking increase in cardiac myocyte NO synthesis, which depends on AMPK and Akt phosphorylations and is associated with transient eNOS phosphorylation and enzyme translocation. Clearly, physiological levels of exogenous H_2O_2 can dynamically modulate NO synthesis and eNOS signaling pathways in cardiac myocytes.

The effects of low concentrations of *exogenous* H_2O_2 on eNOS signaling in cardiac myocytes led us to explore whether *endogenous* H_2O_2 might modulate NO signaling in these cells. We studied responses to the hormone angiotensin II (Ang-II), which increases ROS production in many cell types (21). As shown in Fig. 3*A* and Fig. S2*B*, Ang-II promotes the reversible phosphorylation of eNOS at serines 633 and 1177 in cardiac myocytes. In order to explore a role for endogenous H_2O_2 in modulating the Ang-II response, before adding Ang-II we first incubated the cardiac myocytes with PEG-catalase, a derivatized enzyme that enters cells and rapidly converts H_2O_2 into H_2O and O_2. As can be seen in Fig. 3*A*, preincubation of cardiac myocytes with PEG-catalase abrogates subsequent Ang-II-promoted increase in eNOS phosphorylation at residues serine 1177 and serine 633. We and others previously showed that the β-adrenergic agonist isoproterenol promotes eNOS phosphorylation in cardiac myocytes (8, 22). Fig. 3*B* demonstrates that the isoproterenol-promoted increase in eNOS phosphorylation in cardiac myocytes is unaffected by preincubation with PEG-catalase. The lack of any catalase effect on eNOS phosphorylation following isoproterenol treatment strongly indicates that signaling to eNOS via the β-adrenergic receptor does not involve H_2O_2, whereas the catalase-sensitive Ang-II response appears to depend on generation of intracellular H_2O_2. We used

BIOCHEMISTRY

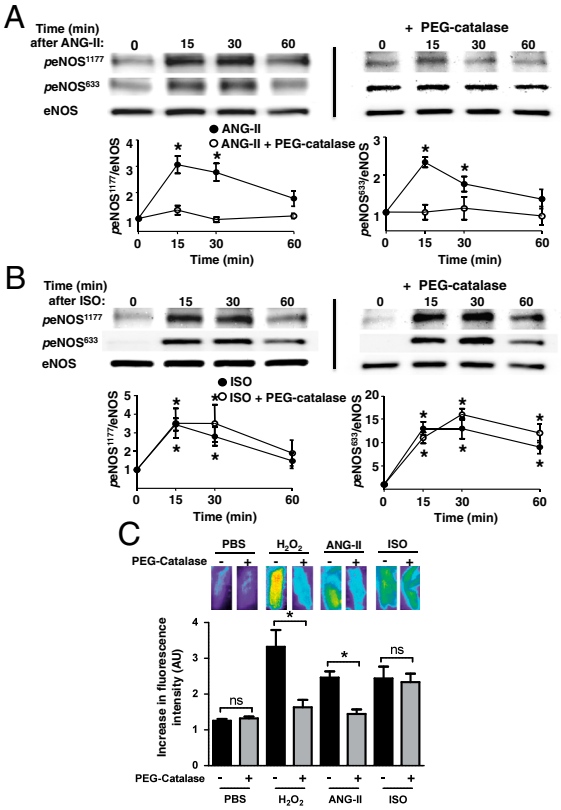

Fig. 3. Differential effects of catalase on angiotensin-II- versus isoproterenol-stimulated eNOS phosphorylation and NO synthesis in cardiac myocytes. Adult mouse cardiac myocytes were incubated overnight with PEG-catalase or vehicle, and treated either with angiotensin II (*A*, Ang-II, 500 nM) or isoproterenol (*B*, ISO, 100 nM) for the indicated times, then harvested, lysed, and analyzed in immunoblots probed with antibodies as indicated. Shown are immunoblots that are representative of three independent experiments that yielded equivalent results. Beneath each immunoblot are shown the results of densitometric analyses from pooled data, showing the increase in eNOS Ser^{1177} or eNOS Ser^{633} phosphorylations in arbitrary units plotted relative to the signal at $t = 0$. (*C*) Effects of PEG-catalase on cardiac myocyte NO synthesis stimulated by H_2O_2, Ang-II, or isoproterenol. Cardiac myocytes isolated from wild-type mice were incubated overnight with PEG-catalase or vehicle, loaded with the Cu_2(FL2E) NO dye, and then treated with H_2O_2 (10 μM), Ang-II (500 nM), or isoproterenol (100 nM), and NO synthesis was quantitated by the change in fluorescence signal between $t = 0$ and $t = 5$ min after adding these compounds. The results shown represent pooled data analyzed from three independent experiments that yielded equivalent results; * indicates $p < 0.05$ comparing control and PEG-catalase-treated cells; ns, not significant; AU, arbitrary units. Each data point represents the mean ± SE derived from three independent experiments. The asterisk * indicates results significant at $p < 0.05$ compared to $t = 0$, analyzed by ANOVA.

the fluorescent NO dye Cu_2(FL2E) to confirm directly that the differential effects of PEG-catalase on receptor-mediated eNOS phosphorylation lead to concordant effects on NO synthesis. As shown in Fig. 3*C*, both Ang-II- and H_2O_2-promoted NO synthesis are blocked by PEG-catalase, whereas the isoproterenol-stimulated increase in NO synthesis is unaffected by PEG-catalase treatment. Treatment of cardiac myocytes with either Ang-II or isoproterenol leads to AMPK phosphorylation (23, 24) (see also Fig. S2 *A*, *C*, and *D*). Importantly, the AMPK inhibitor compound C blocks Ang-II- but not isoproterenol-promoted eNOS phosphorylation (Fig. S2 *B* and *D*). These effects of catalase and compound C indicate a key role for H_2O_2 in modulating the signaling pathway leading from Ang-II to eNOS phosphorylation and NO synthesis in cardiac myocytes.

Ang-II has complex effects on cardiac and vascular function, and the direct effects of Ang-II on cardiac myocyte contractility appear to vary depending upon the specific experimental system being studied (25–28). We found that Ang-II produces a positive inotropic effect on cardiac myocytes isolated from adult mice (Fig. 4). In order to explore a possible role for endogenous H_2O_2 in modulating agonist-dependent contractility, we first incubated them with PEG-catalase prior to and during incubation with isoproterenol or Ang-II. Incubation of cells with PEG-catalase completely blocks the Ang-II-promoted increase in cardiac myocyte contractility, whereas the response to isoproterenol is entirely unaffected by PEG-catalase (Fig. 4). These findings indicate that the effects of Ang-II—but not isoproterenol—on cardiac contractility are dependent on H_2O_2 signaling pathways. This differential involvement of H_2O_2 in agonist-modulated cardiac myocyte contractility parallels the differential role of H_2O_2 in biochemical responses in these cells and helps to establish the involvement of H_2O_2 in physiological responses in the heart.

Our laboratory (29) and others (2, 15, 16, 30) have previously shown that H_2O_2 is a critical modulator of eNOS activation in vascular endothelial cells. However, a role for H_2O_2 regulating NOS isoforms in cardiac myocytes has not been previously reported, and we therefore used complementary experimental approaches to extend our conclusions based on the differential effects of catalase on receptor-mediated eNOS activation. We measured H_2O_2 generation in cardiac myocytes by cloning the recently developed H_2O_2 biosensor HyPer (31, 32) into lentivirus and injecting mice via the tail vein with this recombinant virus; expression of HyPer in cardiac myocytes was documented by immunoblot analyses (Fig. S3). The HyPer2 H_2O_2 biosensor yields an increase in fluorescence that is highly specific for H_2O_2. This biosensor has been characterized extensively in vitro and in cultured cells (29, 31–33). We isolated cardiac myocytes from mice after tail vein injection with the HyPer2 lentivirus and analyzed changes in cell-derived fluorescence after treating the cells with H_2O_2, Ang-II, or isoproterenol (Fig. 5). We observed a prompt increase in HyPer2 fluorescence after addition of 10 μM

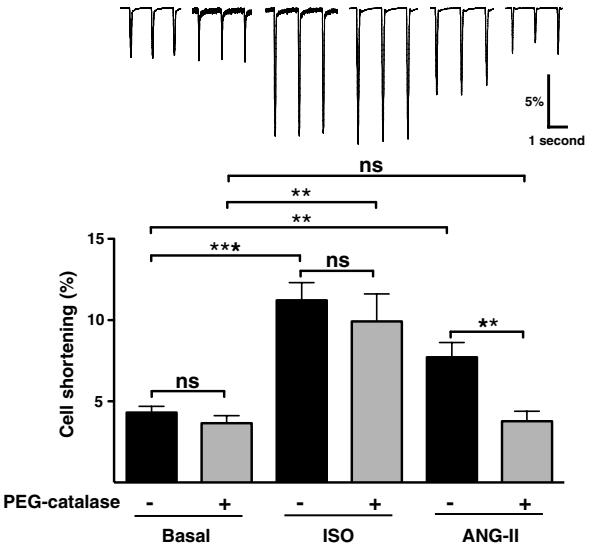

Fig. 4. Differential effects of catalase on agonist-modulated myocyte contractility. (*Upper*) Representative cell shortening traces of adult cardiac myocytes with no treatment (Basal), isoproterenol (ISO), and angiotensin II (ANG-II) treatments in the absence (dark bars) and presence (gray bars) of PEG-catalase (100 units/mL, 2–6 h). The abscissa shows myocyte cell length; deflections from the baseline indicate cell shortening, which was analyzed as the percentage of the baseline resting cell length following treatments as shown. Recordings were performed at 33–35 °C and myocytes were stimulated at 1 Hz, 5–10 V. (*Lower*) Results of pooled data analyzed from three independent experiments (at least three cells per experiment per group) that yielded equivalent results; ** indicates $p < 0.01$, and *** indicates $p < 0.001$; ns, not significant. Each data point represents the mean ± SE analyzed by ANOVA.

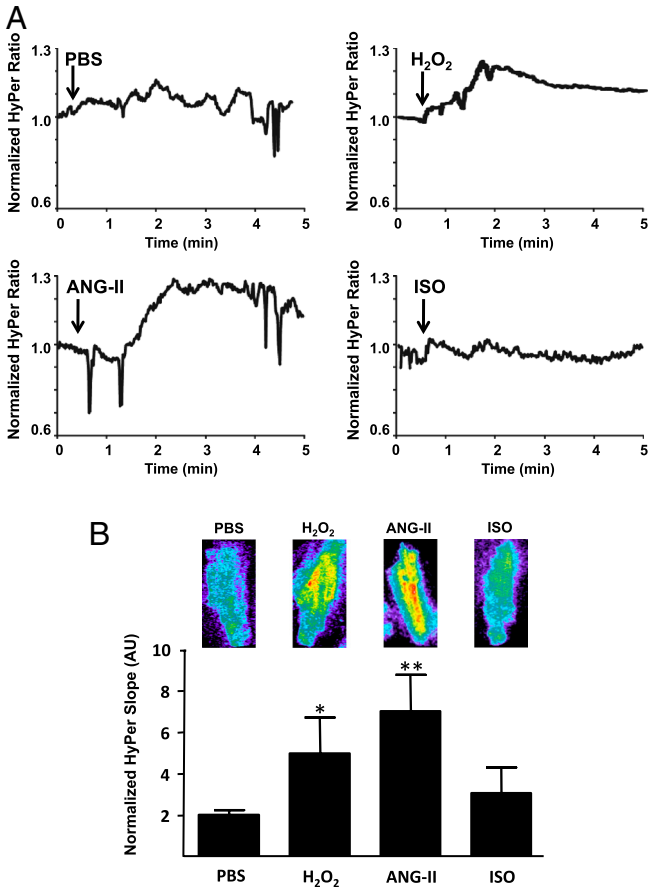

Fig. 5. Detection of H_2O_2 in cardiac myocytes isolated from mice infected with lentivirus expressing the HyPer2 biosensor. Adult mice were injected via the tail vein with lentivirus expressing the HyPer2 H_2O_2 biosensor (10^9 pfu); 2 wk later the mice were euthanized, and cardiac myocytes were isolated and analyzed. (*A*) Representative fluorescence tracings analyzed following cell treatments with phosphate buffer saline, H_2O_2 (10 μM), ANG-II (500 nM), or ISO (100 nM). The bar graph in *B* shows pooled data from three independent experiments, in which the H_2O_2 response is quantitated as the slope of the fluorescence signal in arbitrary units (AU) measured between $t = 0$ and $t = 5$ min after addition of drug; * indicates $p < 0.05$ compared to PBS-treated cells. Also shown in *B* are representative HyPer2 images shown in isolated cardiac myocytes treated as shown. The HyPer2 H_2O_2 image is determined as the YFP500/YFP420 excitation ratio; the grayscale is adjusted to improve contrast.

H_2O_2 to cardiac myocytes isolated from HyPer2 lentivirus-treated mice. Ang-II also promotes a significant increase in HyPer2 fluorescence. By contrast, no increase in HyPer2 fluorescence was observed following addition of isoproterenol under the same conditions that yield increases in NO in response equivalent to those seen in response to Ang-II or H_2O_2. The increase in HyPer2 fluorescence as well as multiple protein phosphorylations following H_2O_2 treatment was abrogated by pretreatment of cardiac myocytes with PEG-catalase (Figs. S4 and S5). These findings using the HyPer2 biosensor extend the conclusions from the catalase experiments. Both Ang-II and isoproterenol are coupled to eNOS phosphorylation and NO synthesis in cardiac myocytes, yet these agonists differentially modulate intracellular H_2O_2 production. H_2O_2 thus serves as a critical messenger molecule that couples Ang-II receptor activation to eNOS activation, but appears to have no significant role for β-adrenergic receptor-mediated signaling to NO synthesis.

The differential roles of eNOS and nNOS in cardiac myocytes are incompletely understood, and the cardiac phenotypes in mice deficient in one or both of these NOS isoforms are subtle in the absence of drugs or diseases (34, 35), despite the roles of NO in modulating cardiac myocyte function (8, 35). The effects of H_2O_2 on nNOS versus eNOS are virtually unexplored in cardiac myocytes. We isolated cardiac myocytes from wild-type, $eNOS^{null}$, or $nNOS^{null}$ mice, and analyzed NO synthesis using the Cu_2(FL2E) fluorescent probe following treatments with H_2O_2, Ang-II, or isoproterenol. The Ang-II- and H_2O_2-promoted increase in NO synthesis are abrogated in cardiac myocytes isolated from $eNOS^{null}$ mice; by contrast, isoproterenol-promoted NO synthesis is maintained—if slightly blunted—compared to wild-type mice (Fig. 6). In contrast, agonist-promoted NO synthesis in cardiac myocytes isolated from $nNOS^{null}$ mice reveal that H_2O_2 and Ang-II responses are sustained, whereas the isoproterenol-promoted increase in myocyte NO synthesis is markedly attenuated in $nNOS^{null}$ mice. These observations suggest that eNOS is the principal if not sole NOS isoform activated by H_2O_2 or by Ang-II, whereas β-adrenergic receptor activation is more importantly coupled to nNOS-dependent NO synthesis. The attenuation of agonist-activated NO synthesis observed in cardiac myocytes form the $eNOS^{null}$ mouse suggests that the eNOS isoform is the principal source of NO in these cells.

Our understanding of the role of ROS in normal physiological signaling is evolving rapidly (3, 33, 36, 37). The present studies define key roles for endogenous H_2O_2 in cardiac myocytes that modulate Ang-II signaling pathways controlling eNOS activation and myocyte contractility. Experiments using the H_2O_2 biosensor HyPer2 and the NO chemical dye Cu_2(FL2E) reveal that Ang-II treatment of cardiac myocytes leads to H_2O_2 synthesis as a prerequisite for NO production and enhanced contractility, whereas β-adrenergic receptor-modulated eNOS activation and contractility responses are independent of H_2O_2 generation. Studies in NOS knockout mouse lines reveal that these two receptor pathways are differentially coupled to nNOS and eNOS, with the

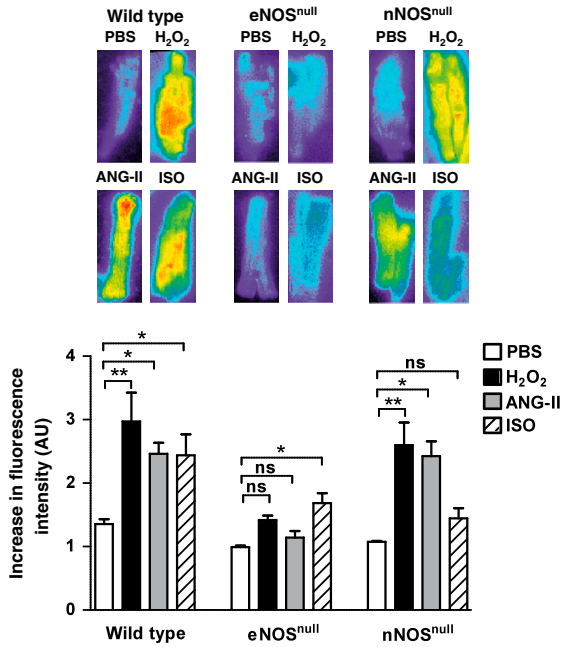

Fig. 6. Differential roles of H_2O_2 in receptor-activated NO synthesis in wild-type, $eNOS^{null}$, and $nNOS^{null}$ cardiac myocytes. Cardiac myocytes were isolated from wild-type, $eNOS^{null}$, or $nNOS^{null}$ mice, and then analyzed for NO production using the Cu_2(FL2E) NO dye following treatments with phosphate buffer saline, H_2O_2 (10 μM), ANG-II (500 nM), or ISO (100 nM), as shown. For each genotype, the values are normalized to the signal seen in the absence of added drug. The results shown represent pooled data analyzed from three independent experiments that yielded equivalent results; * indicates $p < 0.05$ and ** indicates $p < 0.01$ using ANOVA to analyze the effects of drug treatments compared to PBS-treated cells within each genotype; ns, not significant; AU, arbitrary units.

preponderance of the NO synthesized in these cardiac myocytes coming from eNOS and modulated by H_2O_2-dependent pathways. The source of receptor-modulated H_2O_2 in these cells has not been directly determined in these studies. Ang-II is known to activate NADPH oxidases in multiple tissues, yielding superoxide, which may be subsequently metabolized to H_2O_2. However, the molecular mechanisms whereby Ang-II modulates NADPH oxidase isoforms in the heart are incompletely understood; moreover, cardiac myocytes contain multiple NADPH oxidase isoforms that are differentially regulated (38). Experiments studying cardiac myocytes from NADPH isoform-specific knockout mouse models will undoubtedly be informative. Mitochondrial respiration represents another major source of ROS in the heart (36, 38), yet the mechanisms for receptor-dependent modulation of mitochondria-derived H_2O_2 have not been clearly defined. It is interesting to note that NO is itself an inhibitor of mitochondrial oxidative metabolism (1, 36, 37), and it is plausible that eNOS-derived NO could provide a feedback mechanism for the control of mitochondrial ROS generation. Indeed, the heart is an oxidatively active tissue, with a huge flux of oxygen fueling the constant metabolic needs of the cardiac myocytes. The interplay of ROS and reactive nitrogen species reflects a delicate balance in this tissue, with a lively crosstalk between receptors and redox-modulated signaling proteins providing a context both for physiological regulation as well as pathological derangements in disease states characterized by changes in redox balance and alterations in phosphorylation pathways.

Materials and Methods

Materials. The Cu_2(FL2E) NO sensor was prepared as described (9, 10). Polyclonal antibodies directed against phospho-eNOS (Ser1177), phospho-acetyl-CoA carboxylase (ACC) (Ser79), phospho-AMPK (Thr172), phospho-Akt (Ser473), phospho-MEK1/2 (Ser217/221), phospho-Erk1/2 (Thr202/Tyr204), ACC, AMPK, and Akt were from Cell Signaling Technologies. Total eNOS, caveolin 3, and phospho-eNOS (Ser633) monoclonal antibodies were from BD Transduction Laboratories. The GFP antibody Anti-Tag(CGY)FP was from Evrogen. Collagenase type 2 was from Worthington Biochemical. Compound C and piperazine-*N*,*N*′-bis(2-ethanesulfonic acid) (Pipes) were from Calbiochem. Super Signal substrate for chemiluminescence detection and secondary antibodies conjugated with horseradish peroxidase were from Pierce. Tris-buffered saline and phosphate-buffered saline were from Boston Bioproducts. Laminin was from BD Bioscience. Minimum essential medium with Hank's balanced salt solution and glutamine were from Gibco-BRL. Calf serum was from HyClone. Heparin sodium was from APP Pharmaceuticals. All other reagents were from Sigma. Mouse lines C57BL6/J, $eNOS^{null}$, and $nNOS^{null}$ were from Jackson Labs.

Isolation of Adult Mouse Ventricular Myocytes. All animal experimentation was performed according to protocols approved by the Harvard Medical School Committee on Use of Animals in Research. For these studies, 8–10-wk-old, C57BL6/J, $eNOS^{null}$, and $nNOS^{null}$ mice were lightly anesthetized with isoflurane, heparinized (50 units, i.p.), and euthanized. The heart was quickly removed from the chest and retrogradely perfused through the aorta as described (39). Cardiac myocyte isolation methods followed the procedures as described (39), with minor modifications as we have previously reported (22). In brief, enzymatic digestion was initiated by adding collagenase type 2 to the cardiac perfusion solution, followed by the stepwise introduction of $CaCl_2$, after which the heart tissue was minced and the cells were dispersed by trituration, following which the cardiac myocytes were allowed to settle, and then washed, pelleted, counted, and plated.

Cell Culture. Cardiac myocytes were plated in laminin-coated six-well culture dishes (50,000 rod-shaped cells per dish) in plating medium consisted of minimum essential medium with Hank's balanced salt solution, supplemented with calf serum (10% vol/vol), 2,3-butanedione monoxime (10 mM), penicillin-streptomycin (100 units/mL), glutamine (2 mM), and ATP (2 mM). After the cells attached (*ca.* 1 h), the plating medium was changed to culture medium consisting of minimum essential medium with Hank's balanced salt solution, supplemented with bovine serum albumin (1 mg/mL), penicillin-streptomycin (100 units/mL), and glutamine (2 mM), and the cells were cultured for 4 h. For cells cultured overnight, culture medium was supplemented with 2,3-butanedione monoxime (10 mM), insulin (5 μg/mL), transferrin (5 μg/mL), and selenium (5 ng/mL). Cell treatments were performed after culturing the cells either after 4 h or overnight, as indicated. For the H_2O_2 time course experiments, lysates were prepared from cardiac myocytes treated with 25 μM H_2O_2; in the H_2O_2 dose-response experiments, cells were analyzed 15 min after treatment.

Immunoblot Analyses. After drug treatments, cardiac myocytes were washed with PBS and incubated on ice for 20 min in lysis buffer (50 mM Tris·HCl, pH 7.4; 150 mM NaCl; 1% Nonidet P-40; 0.25% sodium deoxycholate; 1 mM EDTA; 2 mM Na_3VO_4; 1 mM NaF; 2 μg/mL leupeptin; 2 μg/mL antipain; 2 μg/mL soybean trypsin inhibitor; and 2 μg/mL lima trypsin inhibitor). Cells were harvested by scraping and then rotated for 15 min at 4 °C. After separation by SDS-PAGE, proteins were electroblotted onto nitrocellulose membranes. After incubating the membranes in 5% nonfat dry milk in Tris-buffered saline with 0.1% (vol/vol) Tween 20 (TBST), membranes were incubated overnight in TBST containing 5% bovine serum albumin plus the specified primary antibody. After four washes (10 min each) with TBST, the membranes were incubated for 1 h with a horseradish peroxidase-labeled goat antirabbit or antimouse immunoglobulin secondary antibody in TBST containing 1% milk. The membranes were washed four additional times in TBST, then incubated with a chemiluminescent reagent according to the manufacturer's protocols (SuperSignal West Femto), and digitally imaged in a chemiluminescence imaging system (Alpha Innotech Corporation). Quantitative analyses of the chemiluminescent signals were performed using an AlphaEaseFC software (Alpha Innotech). For quantitative analyses of dose-response or time course immunoblot experiments, the signal is normalized to the value obtained in the absence of added drug or at $t = 0$, respectively. Where indicated in the experiments showing quantitative densitometry analyzed in immunoblots, the ordinate is in arbitrary units.

Intracellular Nitric Oxide Imaging. Cardiac myocytes harvested from at least three independent preparations were analyzed. The signal from the NO sensor is analyzed as the slope of the fluorescence increase seen following the addition of agonist or vehicle; there was variation in the "basal fluorescence level" between experimental preparations because of the differences in loading of the NO dye from prep to prep. Cells were cultured on coverslips and loaded with 5 μM Cu_2(FL2E) NO dye (9) for 1 h in culture medium at 37 °C and 2% CO_2. Coverslips were then placed in an onstage incubator (Tokai) on the microscope in a low-volume glass-covered recording chamber. Fluorescence signals were analyzed by using a Hamamatsu Orca CCD camera (Hamamatsu) coupled to an inverted microscope (IX81; Olympus) at 470 nm.

Immunohistochemistry. Cardiac myocytes plated on glass bottom dishes (Mattek) were immersed in 4% paraformaldehyde for 20 min, rinsed twice with PBS, permeabilized in 0.1% Triton X-100 for 45 min, and blocked with 10% goat serum overnight. Immunoreactive eNOS and caveolin 3 were colocalized using confocal microscopy. After incubating with both primary antibodies (in blocking solution at 4 °C), samples were washed three times in PBS for 10 min. The Cav-3 primary antibody was localized by immunofluorescent detection with a secondary Alexa Fluor green (488)-tagged goat antirabbit antibody (1:200 dilution, 1-h incubation; Molecular Probes), and eNOS primary antibody was detected with a secondary Alexa Fluor red (568)-tagged goat antimouse antibody (1:200 dilution, 1-h incubation; Molecular Probes). Samples were washed three times in PBS for 10 min to remove excess secondary antibody and then mounted on slides using medium containing 4′,6-diamidino-2-phenylindole as nuclear counterstain. Microscopic analysis of samples was performed using an Olympus IX81 inverted microscope in conjunction with a DSU spinning disk confocal system equipped with a Hamamatsu Orca ER cooled-CCD camera. Images were acquired using a 40× differential interference contrast oil immersion objective lens and analyzed using Metamorph software from Universal Imaging, Inc.

Myocyte Contractility. Myocytes were placed in a stimulation chamber on an inverted Nikon microscope stage and continuously bathed at 33–35 °C in Tyrode's solution, pH 7.45, containing 1.25 mM $CaCl_2$ and analyzed using instrumentation from IonOptix. Myocytes were field-stimulated (MyoPacer Field Stimulator, IonOptix) at 1 Hz, 5–10 V. Cell length was recorded with a video edge detector coupled to a camera (IonOptix MyoCam-S). Cell shortening analysis was performed using IonWizard Core Analysis software in myocytes without any treatment or after 5 min of isoproterenol or after 15 min of Ang-II treatments. In some studies, myocytes were pretreated with PEG-catalase (100 units/mL) for at least 2 h before isoproterenol or Ang-II treatments. Cell shortening was expressed as percent shortening relative to the resting cell length.

HyPer2 Lentivirus Cloning and Tail Vein Injection. The coding sequence of HyPer2 was cloned into the pWPXL lentiviral expression plasmid downstream of the EF1-α promoter. Recombinant vesicular stomatitis virus-glycoprotein pseudo-typed lentivirus particles were generated in HEK293T cells by transfection of the envelope:packaging:transgene plasmids at a 1:1:1.5 ratio with Fugene6 (Roche) according to the manufacturer's protocol. The viral titer was determined with Lenti-X GoStix (Clontech), and virus particles were concentrated by polyethylene glycol precipitation with PEG-it solution (SBI Bioscience), according to the manufacturer's protocol. The virus pellet was resuspended in PBS and stored at −80 °C. Final titer was determined by serial dilution and fluorescence microscopy.

Expression of HyPer2 Lentivirus in Cardiac Myocytes After Tail Vein Injection. HyPer2 lentivirus was infused through the tail vein (250 μL of 10^8 pfu/mL) of adult male mice (8–10 wk old). Fourteen days after injection of virus (or saline control), mice were euthanized, and cardiac myocytes were isolated and cultured overnight as described above. The next day, cells were placed in the microscope stage incubator (Tokai), and HyPer2 fluorescence was excited with 420/40 and with 500/16 band-pass excitation filters; corresponding YFP emission was acquired every 5 s for 10 min using a 535/30 band-pass emission filter. For calculating HyPer ratio images, CFP and YFP images were acquired; after background subtraction, the HyPer2 signal was quantitated as described above and as we have previous reported (27).

Spectroscopic Methods and Reagents. Solution fluorescence spectra were measured on a Quanta Master 4 L-format scanning spectrofluorimeter (Photon Technology International) at 37.0 ± 0.1 °C. Fluorescence measurements were made under anaerobic conditions, with cuvette solutions prepared in an inert atmosphere glove box. FL2A was prepared as described (9). Nitric oxide was purchased from Airgas and purified as described previously. Solutions were buffered to pH 7.0 with 50 mM Pipes and 100 mM KCl. To test the response of Cu_2FL2A (the product of Cu_2FL2E after hydrolysis by intracellular esterases), the background fluorescence of a 1.0 μM Cu_2FL2A solution in Pipes buffer was measured (λex = 470 nm, λscan = 475–650 nm), after which 0, 1, 10, 50, or 100 equiv of H_2O_2 were added. After incubation at 37 °C for 30 min, a second fluorescence spectrum was acquired. Finally, 1,300 equiv of NO was added and incubated for 30 min at 37 °C, after which a third fluorescence spectrum was measured. To test the influence of H_2O_2 on the fluorescence of Cu_2FL2A after reaction with NO, a 1.0-μM solution of Cu_2FL2A was treated with 1,300 equiv of NO and incubated for 30 min at 37 °C. After measurement of the resultant fluorescence spectrum, the solution was treated with 100 equiv of H_2O_2, incubated for 30 min at 37 °C, and a final fluorescence spectrum was acquired. These results, which are shown in Fig. S6, document that Cu_2FL2A is able to detect NO in the presence of H_2O_2.

ACKNOWLEDGMENTS. We thank Drs. Ruqin Kou, Takashi Shiroto, and Yan Zhonghua for critical discussions. This work was supported in part by National Institutes of Health Grants GM36259, HL46457, HL48743 (to T.M.), and K99GM092970 (to M.D.P.), and National Science Foundation Grant CHE-0907905 (to S.J.L.); by an American Diabetes Association/Takeda Cardiovascular Postdoctoral Fellowship Award (to J.L.S.); and by a postdoctoral fellowship from the Fonds National de Recherche, Luxembourg (to H.K.).

1. Stocker R, Keaney JF, Jr (2004) Role of oxidative modifications in atherosclerosis. *Physiol Rev* 84:1381–1478.
2. Storz P (2006) Reactive oxygen species-mediated mitochondria-to-nucleus signaling: A key to aging and radical-caused diseases. *Sci STKE* 2006:re3.
3. Rudolph TK, Freeman BA (2009) Transduction of redox signaling by electrophile-protein reactions. *Sci Signal* 2:re7.
4. Cai H (2005) NAD(P)H oxidase-dependent self-propagation of hydrogen peroxide and vascular disease. *Circ Res* 96:818–822.
5. D'Autreaux B, Toledano MB (2007) ROS as signalling molecules: Mechanisms that generate specificity in ROS homeostasis. *Nat Rev Mol Cell Biol* 8:813–824.
6. Cary SP, Winger JA, Derbyshire ER, Marletta MA (2006) Nitric oxide signaling: No longer simply on or off. *Trends Biochem Sci* 31:231–239.
7. Mustafa AK, Gadalla MM, Snyder SH (2009) Signaling by gasotransmitters. *Sci Signal* 2:re2.
8. Balligand JL, Feron O, Dessy C (2009) eNOS activation by physical forces: From short-term regulation of contraction to chronic remodeling of cardiovascular tissues. *Physiol Rev* 89:481–534.
9. McQuade LE, et al. (2010) Visualization of nitric oxide production in the mouse main olfactory bulb by a cell-trappable copper(II) fluorescent probe. *Proc Natl Acad Sci USA* 107:8525–8530.
10. McQuade LE, Pluth MD, Lippard SJ (2010) Mechanism of nitric oxide reactivity and fluorescence enhancement of the NO-specific probe CuFL1. *Inorg Chem* 49:8025–8033.
11. Dudzinski DM, Igarashi J, Greif D, Michel T (2006) The regulation and pharmacology of endothelial nitric oxide synthase. *Annu Rev Pharmacol Toxicol* 46:235–276.
12. Chen ZP, et al. (1999) AMP-activated protein kinase phosphorylation of endothelial NO synthase. *FEBS Lett* 443:285–289.
13. Chen Z, et al. (2009) AMP-activated protein kinase functionally phosphorylates endothelial nitric oxide synthase Ser633. *Circ Res* 104:496–505.
14. Levine YC, Li GK, Michel T (2007) Agonist-modulated regulation of AMP-activated protein kinase (AMPK) in endothelial cells. Evidence for an AMPK → Rac1 → Akt → endothelial nitric-oxide synthase pathway. *J Biol Chem* 282:20351–20364.
15. Thomas SR, Chen K, Keany JF, Jr (2002) Hydrogen peroxide activates endothelial nitric-oxide synthase through coordinated phosphorylation and dephosphorylation via a phosphoinositide 3-kinase-dependent signaling pathway. *J Biol Chem* 277:6017–6024.
16. Cai H, McNally JS, Weber M, Harrison DG (2004) Oscillatory shear stress upregulation of endothelial nitric oxide synthase requires intracellular hydrogen peroxide and CaMKII. *J Mol Cell Cardiol* 37:121–125.
17. Kim MS, et al. (2004) Anti-obesity effects of alpha-lipoic acid mediated by suppression of hypothalamic AMP-activated protein kinase. *Nat Med* 10:727–733.
18. Gonzalez E, Kou R, Lin AJ, Golan DE, Michel T (2002) Subcellular targeting and agonist-induced site-specific phosphorylation of endothelial nitric-oxide synthase. *J Biol Chem* 277:39554–39560.
19. Feron O, et al. (1996) Endothelial nitric oxide synthase targeting to caveolae. Specific interactions with caveolin isoforms in cardiac myocytes and endothelial cells. *J Biol Chem* 271:22810–22814.
20. Belhassen L, Feron O, Kaye DM, Michel T, Kelly RA (1997) Regulation by cAMP of post- translational processing and subcellular targeting of endothelial nitric-oxide synthase (type 3) in cardiac myocytes. *J Biol Chem* 272:11198–11204.
21. Garrido AM, Griendling KK (2009) NADPH oxidases and angiotensin II receptor signaling. *Mol Cell Endocrinol* 302:148–158.
22. Sartoretto JL, et al. (2009) Regulation of VASP phosphorylation in cardiac myocytes: Differential regulation by cyclic nucleotides and modulation of protein expression in diabetic and hypertrophic heart. *Am J Physiol Heart Circ Physiol* 297:H1697–1710.
23. Jaswal JS, et al. (2010) Isoproterenol stimulates 5′-AMP-activated protein kinase and fatty acid oxidation in neonatal hearts. *Am J Physiol Heart Circ Physiol* 299:H1135–1145.
24. Nagata D, et al. (2004) AMP-activated protein kinase inhibits angiotensin II-stimulated vascular smooth muscle cell proliferation. *Circulation* 110:444–451.
25. Rajagopal K, et al. (2006) Beta-arrestin2-mediated inotropic effects of the angiotensin II type 1A receptor in isolated cardiac myocytes. *Proc Natl Acad Sci USA* 103:16284–16289.
26. Palomeque J, et al. (2006) Angiotensin II-induced negative inotropy in rat ventricular myocytes: Role of reactive oxygen species and p38 MAPK. *Am J Physiol Heart Circ Physiol* 290:H96–106.
27. Lefroy DC, et al. (1996) Angiotensin II and contraction of isolated myocytes from human, guinea pig, and infarcted rat hearts. *Am J Physiol* 270:H2060–2069.
28. Liang W, et al. (2010) Role of phosphoinositide 3-kinase α, protein kinase C, and L-type Ca^{2+} channels in mediating the complex actions of angiotensin II on mouse cardiac contractility. *Hypertension* 56:422–429.
29. Jin BY, Sartoretto JL, Gladyshev VN, Michel T (2009) Endothelial nitric oxide synthase negatively regulates hydrogen peroxide-stimulated AMP-activated protein kinase in endothelial cells. *Proc Natl Acad Sci USA* 106:17343–17348.
30. Cai H, et al. (2002) NAD(P)H oxidase-derived hydrogen peroxide mediates endothelial nitric oxide production in response to angiotensin II. *J Biol Chem* 277:48311–48317.
31. Belousov VV, et al. (2006) Genetically encoded fluorescent indicator for intracellular hydrogen peroxide. *Nat Methods* 3:281–286.
32. Markvicheva KN, et al. (2011) A genetically encoded sensor for H(2)O(2) with expanded dynamic range. *Bioorg Med Chem* 19:1079–1084.
33. Niethammer P, Grabher C, Look AT, Mitchison TJ (2009) A tissue-scale gradient of hydrogen peroxide mediates rapid wound detection in zebrafish. *Nature* 459:996–999.
34. Tsutsui M, Shimokawa H, Otsuji Y, Yanagihara N (2010) Pathophysiological relevance of NO signaling in the cardiovascular system: Novel insight from mice lacking all NO synthases. *Pharmacol Ther* 128:499–508.
35. Feron O, et al. (1998) Modulation of the endothelial nitric-oxide synthase-caveolin interaction in cardiac myocytes. Implications for the autonomic regulation of heart rate. *J Biol Chem* 273:30249–30254.
36. Nathan C (2003) Specificity of a third kind: Reactive oxygen and nitrogen intermediates in cell signaling. *J Clin Invest* 111:769–778.
37. Moncada S, Erusalimsky JD (2002) Does nitric oxide modulate mitochondrial energy generation and apoptosis. *Nat Rev Mol Cell Biol* 3:214–220.
38. Maejima Y, et al. (2011) Regulation of myocardial growth and death by NADPH oxidase. *J Mol Cell Cardiol* 50:408–416.
39. Sakai K, Akima M, Tsuyama K (1983) Evaluation of the isolated perfused heart of mice, with special reference to vasoconstriction caused by intracoronary acetylcholine. *J Pharmacol Methods* 10:263–270.

Supporting Information

Sartoretto et al. 10.1073/pnas.1111331108

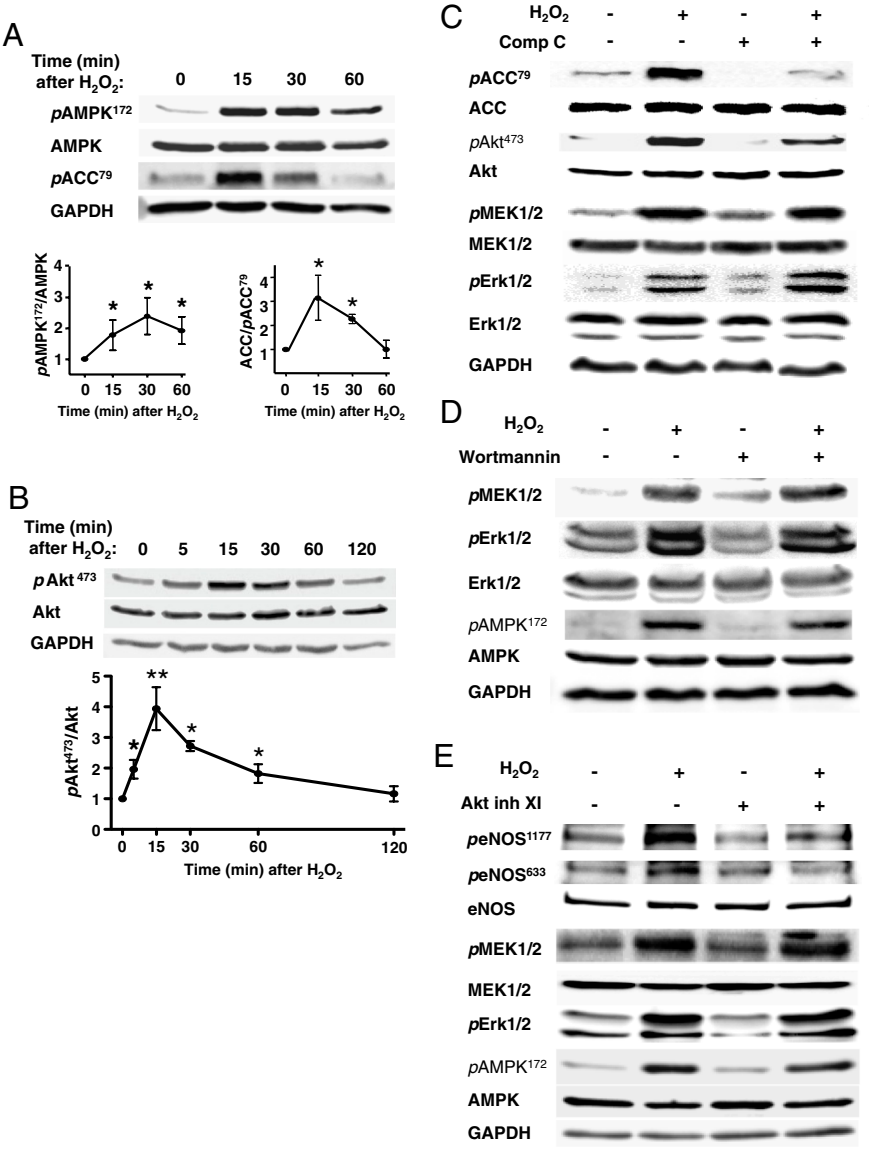

Fig. S1. H_2O_2-promoted phosphorylation of AMP-activated protein kinase (AMPK) and Akt in cardiac myocytes. (*A*) Time course for H_2O_2-stimulated AMPK phosphorylation at threonine 172 (pAMPK^{172}); a representative experiment is shown above and pooled data from three experiments are presented below; * indicates $p < 0.05$. (*B*) Time course for H_2O_2-induced Akt phosphorylation at serine 473 (pAkt^{473}); a representative experiment is shown above and pooled data from three experiments are presented below; * indicates $p < 0.05$ and ** indicates $p < 0.01$. (*C*) Results of immunoblot analyses performed in adult cardiac myocyte lysates prepared from cells incubated with the AMPK inhibitor compound C (Comp C, 20 μM, 30 min) before treatment with H_2O_2 (25 μM, 15 min). Immunoblots were probed with antibodies directed against phospho-acetyl-CoA carboxylase (ACC) Ser^{79}, phospho-Akt Ser^{473}, phospho-mitogen-activated protein kinase kinase–ERK1/2 (MEK1/2) Ser$^{217/221}$, phospho-Erk1/2 Thr^{202}/Tyr^{204}, ACC, Akt, MEK1/2, Erk1/2, or GAPDH, as indicated. The experiment shown is representative of three independent experiments that yielded similar results. (*D*) Results of immunoblot analyses performed in adult cardiac myocyte lysates prepared from cells incubated with the PI3K inhibitor wortmannin (1 μM, 30 min) before treatment with H_2O_2 (25 μM, 15 min). Immunoblots were probed with antibodies as indicated. The experiment shown is representative of three independent experiments that yielded similar results. (*E*) Results of immunoblot analyses performed in cell lysates prepared from cardiac myocyte that were incubated with the Akt inhibitor XI (Akt inh XI, 1 μM, 30 min) prior treatment with H_2O_2 (25 μM, 15 min); blots were probed with antibodies as shown. The experiment shown is representative of three independent experiments.

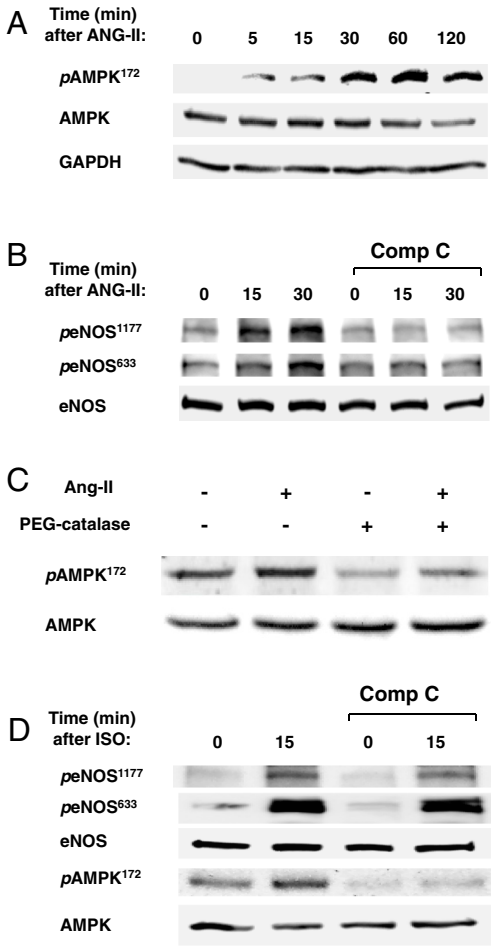

Fig. S2. (*A*) Angiotensin-II-promoted AMP-activated protein kinase (AMPK) phosphorylation. This figure shows the time course for angiotensin-II-mediated AMPK phosphorylation. Shown are the results of immunoblots analyzed in lysates prepared from adult cardiac myocytes treated with angiotensin II (ANG-II, 500 nM) for the indicated times. Cell lysates were analyzed in immunoblots probed using antibodies directed against phospho-AMPK Thr^{172}, AMPK, and GAPDH, as indicated. The experiment shown is representative of three independent experiments that yielded similar results. (*B*) Effects of the AMPK inhibitor compound C on angiotensin-II-promoted eNOS phosphorylation. This figure shows the results of immunoblot analyses performed in adult cardiac myocyte lysates prepared from cells incubated with the AMPK inhibitor compound C (Comp C, 20 μM, 30 min) before treatment with angiotensin II (ANG-II, 500 nM) for the indicated times. Immunoblots were probed with antibodies directed against phospho-endothelial isoform of nitric oxide synthase (eNOS) Ser^{1177}, phospho-eNOS Ser^{633}, or eNOS, as indicated. The experiment shown is representative of three independent experiments. (*C*) Effects of PEG-catalase on angiotensin-II-promoted AMPK phosphorylation. This figure shows the results of immunoblot analyses performed in adult cardiac myocyte lysates prepared from cells incubated with PEG-catalase before treatment with angiotensin II (ANG-II, 500 nM) for 15 min. Immunoblots were probed with antibodies directed against phospho-AMPK, as described in detail in *Materials and Methods*. (*D*) Effects of the AMPK inhibitor compound C on isoproterenol-promoted eNOS phosphorylation. *D* shows the results of immunoblot analyses performed in cell lysates prepared from cardiac myocyte that were incubated with the AMPK inhibitor compound C (Comp C, 20 μM, 30 min) before treatment with isoproterenol (ISO 100 nM, 15 min); blots were probed with antibodies as shown. The experiment shown is representative of three independent experiments.

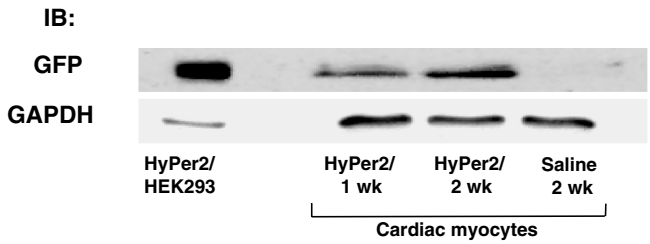

Fig. S3. Expression of the recently developed H_2O_2 biosensor HyPer2 in mouse cardiac myocytes. Shown is a representative immunoblot (IB) of cardiac myocytes isolated from mice 1 or 2 wk following tail vein injection of HyPer2 lentivirus; myocytes isolated from saline-injected mice serve as a negative control, and HEK293 cells infected with the HyPer2 lentivirus serve as a positive control. Immunoblots were probed with antibodies as indicated, directed against either GFP [Anti-Tag(CGY)FT antibody] to detect HyPer2, or with GAPDH antibodies as a loading control.

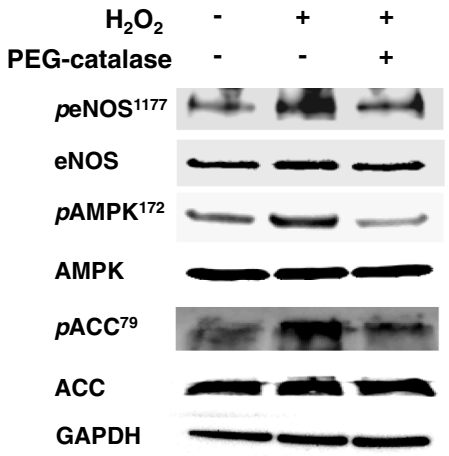

Fig. S4. Effects of PEG-catalase on H_2O_2-promoted increase in protein phosphorylation. This figure shows the results of immunoblot analyses performed in adult cardiac myocyte lysates prepared from cells either incubated or not with PEG-catalase (100 units/mL, 1 h) before treatment with H_2O_2 (25 μM, 15 min). Blots were probed with antibodies against phospho-endothelial isoform of nitric oxide synthase (eNOS) Ser^{1177}, phospho-AMP-activated protein kinase (AMPK) Thr^{172}, phospho-acetyl-CoA carboxylase (ACC) Ser^{79}, phospho-mitogen-activated protein kinase kinase–ERK1/2 (MEK1/2) Ser$^{217/221}$, phospho-Erk1/2 Thr^{202}/Tyr^{204}, ACC, MEK1/2, Erk1/2, or GAPDH as indicated. The experiment shown is representative of three independent experiments that yielded similar results.

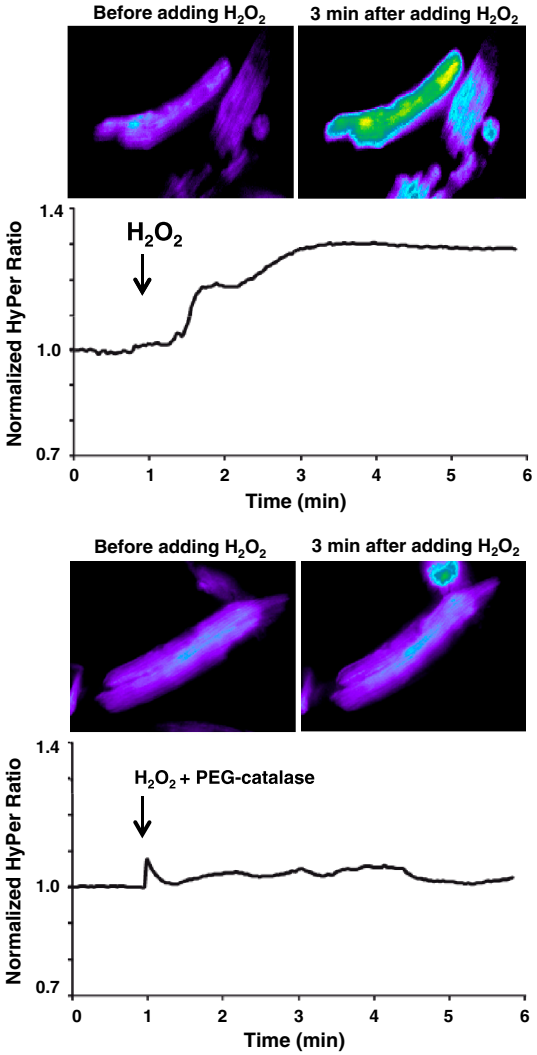

Fig. S5. Effects of PEG-catalase on H_2O_2-promoted increase in the recently developed H_2O_2 biosensor HyPer2 fluorescence. Adult mice were injected via the tail vein with lentivirus expressing the HyPer2 biosensor; 2-wk later the mice were euthanized following cardiac myocytes isolation. Cultured cells were treated with H_2O_2 (10 μM), in some studies myocytes were pretreated with PEG-catalase (100 units/mL) for at least 2 h before H_2O_2 treatment. (*Upper*) Representative HyPer2 images in isolated cardiac myocytes before adding H_2O_2 or 3 min after adding H_2O_2. (*Lower*) Representative fluorescence tracings analyzed following cell treatment with H_2O_2 (10 μM). The HyPer2 H_2O_2 image is determined as the YFP500/YFP420 excitation ratio; the grayscale is adjusted to improve contrast.

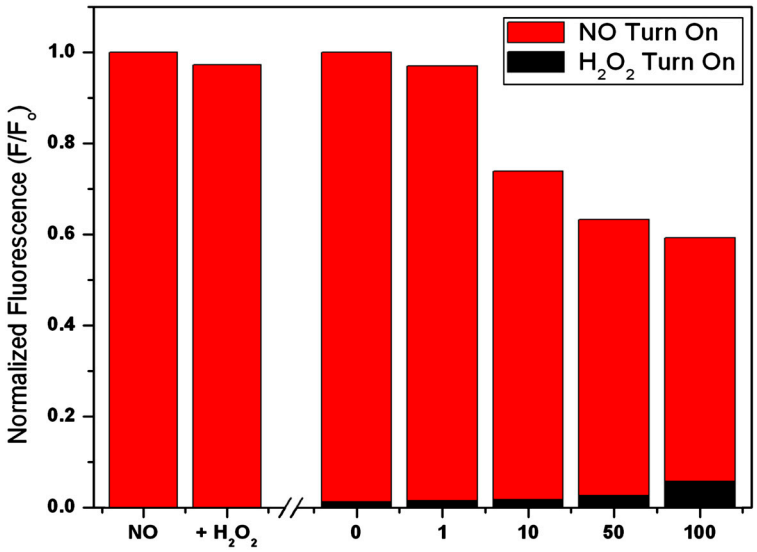

Fig. S6. Cu_2FL2A detects NO in the presence of H_2O_2. The two left bars show the integrated fluorescence of Cu_2FL2A after reaction with 1,300 equivalents of NO either after a 30 min incubation ("NO"), or followed by the addition of 100 equivalents of H_2O_2 and incubation for a further 30 min ("+H_2O_2"). The right bars shows the integrated fluorescence of Cu_2FL2A following the addition of the indicated amounts of H_2O_2 for 30 min (shown in black at each H_2O_2 concentration), followed by the addition of 1,300 equivalents of NO and incubation for a further 30 min (in red). The experimental conditions are described in detail *Materials and Methods*.